articles

Targeting Beta-3 Integrin Using a Linear Hexapeptide Labeled with a Near-Infrared Fluorescent Molecular Probe

**Sharon Bloch,[†] Baogang Xu,[†] Yunpeng Ye,[†] Kexian Liang,[†]
Gregory V. Nikiforovich,[‡] and Samuel Achilefu*,[†]**

*Department of Radiology and Department of Biochemistry and Molecular Biophysics,
Washington University School of Medicine, St. Louis, Missouri*

Abstract: Biomolecules containing the RGD peptide sequence are known to bind integrins with high affinity. Studies of hexa-and hepta-peptides labeled with a near-infrared fluorescent probe (cypate) showed that rearranging the glycine in a linear RGD peptide sequence to form the GRD analogue favored the uptake of the GRD compound by $\alpha_v\beta_3$ integrin receptor (ABIR)-positive A549 tumor cells and tissue. The internalization of the GRD compound in A549 cells and tumor uptake in mice were inhibited by ABIR-avid peptides, suggesting its recognition by this receptor. Further studies with functional blocking antibodies and β_3 knockout cells revealed that β_3 integrin mediates the internalization of the cypate-GRD peptide. Molecular modeling studies supported preferential interaction of the probe with the β_3 subunit of integrins relative to the α_v subunit. The results demonstrate that the cypate-GRD peptide targets β_3 integrin, thereby providing a strategy to monitor drug delivery and efficacy, and physiopathologic processes mediated by this protein.

Keywords: Integrin; cancer; near-infrared; imaging; molecular probe

Introduction

Integrins are a large family of heterodimeric transmembrane receptors that mediate cell–cell and cell–matrix interactions. They play key roles in tumor invasion, metastasis, and neovascularization. These proteins associate as $\alpha\beta$ heterodimers in native environment, where the α and β subunits control distinct but complementary physiological functions.[1,2] Currently, 18 α and 8 β integrin subunits have

been identified, with each β subunit associating with different α proteins. The β_3 subunit has been shown to form $\alpha_{IIb}\beta_3$ and $\alpha_v\beta_3$ heterodimers.[3,4] Various anti-angiogenic drugs[5–8] and tumor imaging agents[9–13] have been developed to target the $\alpha_v\beta_3$ integrin receptor (ABIR) because of its overexpres-

* Corresponding author. Address: Department of Radiology, Washington University School of Medicine, Campus Box 8225, 4525 Scott Avenue, St. Louis, MO 63110. Tel: 314-362-8599. Fax: 314-747-5191. E-mail: achilefu@mir.wustl.edu.

† Department of Radiology.

‡ Department of Biochemistry and Molecular Biophysics.

(1) Arnaout, M. A. Integrin structure: new twists and turns in dynamic cell adhesion. *Immunol. Rev.* **2002**, *186*, 125–140.

(2) Arnaout, M. A.; Goodman, S. L.; Xiong, J. P. Coming to grips with integrin binding to ligands. *Curr. Opin. Cell Biol.* **2002**, *14*, 641–651.

(3) Felding-Habermann, B.; Cheresh, D. A. Vitronectin and its receptors. *Curr. Opin. Cell Biol.* **1993**, *5*, 864–868.

(4) Stupack, D. G. Integrins as a distinct subtype of dependence receptors. *Cell Death Differ.* **2005**, *12*, 1021–1030.

(5) Liekens, S.; De Clercq, E.; Neyts, J. Angiogenesis: regulators and clinical applications. *Biochem. Pharmacol.* **2001**, *61*, 253–270.

(6) Brooks, P. C.; Montgomery, A. M. P.; Rosenfeld, M.; Reisfeld, R. A.; Hu, T. H.; Klier, G.; Cheresh, D. A. Integrin Alpha(V)-Beta(3) Antagonists Promote Tumor-Regression by Inducing Apoptosis of Angiogenic Blood-Vessels. *Cell* **1994**, *79*, 1157–1164.

(7) Brooks, P. C.; Stromblad, S.; Klemke, R.; Visscher, D.; Sarkar, F. H.; Cheresh, D. A. Antiintegrin Alpha-V–Beta-3 Blocks Human Breast-Cancer Growth and Angiogenesis in Human Skin. *J. Clin. Invest.* **1995**, *96*, 1815–1822.

sion in many pathophysiological processes. In particular, the β_3 integrin is associated with a number of cancers, including prostate,[14] cervical,[15] breast,[16] stomach,[17] melanomas,[18] and glioblastomas,[19] However, only a limited number of studies have targeted the β_3 integrin for diagnostic and therapeutic interventions, and very little is known about β_3-specific synthetic peptides.

Biomolecules and synthetic compounds containing the arginine−glycine−aspartic acid (RGD) peptide sequence are known to bind ABIR and related integrin heterodimers with high affinity.[9,20] In a recent study, we demonstrated that rearrang-

ing the glycine in a linear RGD peptide sequence and labeling the resultant GRD peptide with a near-infrared (NIR) fluorescent dye (cypate, **1**) afforded an imaging agent that was specifically retained by ABIR-positive A549 tumor cells and tissue.[21]

In this paper, we provide experimental evidence that cellular internalization and tumor uptake of the GRD peptide, cypate-GRDSPK−OH, (**2**) by ABIR-positive tumor cells are mediated by the initial association of the probe with the β_3 integrin subunit. Molecular modeling also supports the preferential binding of the compound to the β_3 integrin relative to the α_v subunit. Because the β_3 integrin is involved in many pathologic conditions, the GRD peptide could be used to target this protein for imaging and therapeutic applications, especially for drug-development purposes where treatment response can be monitored with a fluorescent- or radio-labeled GRD peptide.

Experimental Section

Chemistry. All reagents and solvents were obtained from commercial sources and used without further purification. Amino acids were purchased from Novabiochem (San Diego, CA). ABIR-avid peptide **5** was purchased from Peptide International (Louisville, KY) and used for the blocking studies. The NIR fluorescent dye **1** was prepared as we reported previously.[22] Purification and analysis of the new peptides were performed on an HPLC system equipped with a tunable UV−visible detector. Analytical (flow rate = 0.5 mL/min) and semipreparative (flow rate = 10 mL/min) reverse phase-HPLC were performed on C-18 columns and detected at 214 and 254 nm. The gradient elution protocol ranged from a mixture of 95% A and 5% B to 30% A and 70% B in 30 min, where solvent A is 0.1% aqueous TFA and solvent B is acetonitrile containing 0.1% of a solution of 0.1% aqueous TFA. Mass spectra were obtained using a Shimadzu mass spectrometer (LCMS-2010A) in the positive electrospray mode. The HPLC purities of all compounds used for the in vivo and in vitro studies were generally >95%.

Peptide Synthesis and Conjugation with Fluorescent Molecular Probes. The linear peptides were prepared with ACT APEX 396 peptide synthesizer by standard 9-fluorenylmethoxycarbonyl (Fmoc) protocol,[23] as described previously.[24,25] Conjugation of the molecular probes with peptides was performed on solid supports. The cyclic peptide was

(8) Allman, R.; Cowburn, P.; Mason, M. In vitro and in vivo effects of a cyclic peptide with affinity for the alpha v beta 3 integrin in human melanoma cells. *Eur. J. Cancer* **2000**, *36*, 410−422.

(9) Haubner, R.; Wester, H. J.; Burkhart, F.; Senekowitsch-Schmidtke, R.; Weber, W.; Goodman, S. L.; Kessler, H.; Schwaiger, M. Glycosylated RGD-containing peptides, tracer for tumor targeting and angiogenesis imaging with improved biokinetics. *J. Nucl. Med.* **2001**, *42*, 326−336.

(10) van Hagen, P. M.; Breeman, W. A. P.; Bernard, H. F.; Schaar, M.; Mooij, C. M.; Srinivasan, A.; Schmidt, M. A.; Krenning, E. P.; de Jong, M. Evaluation of a radiolabeled cyclic DTPA-RGD analogue for tumour imaging and radionuclide therapy. *Int. J. Cancer* **2000**, *90*, 186−198.

(11) Sivolapenko, G. B.; Skarlos, D.; Pectasides, D.; Stathopoulou, E.; Milonakis, A.; Sirmalis, G.; Stuttle, A.; Courtenay-Luck, N. S.; Konstantinides, K.; Epenetos, A. A. Imaging of metastatic melanoma utilising a technetium-99m labelled RGD-containing synthetic peptide. *Eur. J. Nucl. Med.* **1998,** *25*, 1383−1389.

(12) Haubner, R.; Wester, H. J.; Reuning, U.; Senekowitsch-Schmidtke, R.; Diefenbach, B.; Kessler, H.; Stocklin, G.; Schwaiger, M. Radiolabeled alpha(v)beta(3) integrin antagonists: A new class of tracers for tumor targeting. *J. Nucl. Med.* **1999**, *40*, 1061−1071.

(13) Janssen, M. L.; Oyen, W. J.; Dijkgraaf, I.; Massuger, L. F.; Frielink, C.; Edwards, D. S.; Rajopadhye, M.; Boonstra, H.; Corstens, F. H.; Boerman, O. C. Tumor targeting with radiolabeled alpha(v)beta(3) integrin binding peptides in a nude mouse model. *Cancer Res.* **2002**, *62*, 6146−6151.

(14) Wang, X.; Ferreira, A. M.; Shao, Q.; Laird, D. W.; Sandig, M. Beta3 integrins facilitate matrix interactions during transendothelial migration of PC3 prostate tumor cells. *Prostate* **2005**, *63*, 65−80.

(15) Gruber, G.; Hess, J.; Stiefel, C.; Aebersold, D. M.; Zimmer, Y.; Greiner, R. H.; Studer, U.; Altermatt, H. J.; Hlushchuk, R.; Djonov, V. Correlation between the tumoral expression of beta 3-integrin and outcome in cervical cancer patients who had undergone radiotherapy. *Br. J. Cancer* **2005**, *92*, 41−46.

(16) Pignatelli, M.; Cardillo, M. R.; Hanby, A.; Stamp, G. W. H. Integrins and Their Accessory Adhesion Molecules in Mammary Carcinomas − Loss of Polarization in Poorly Differentiated Tumors. *Hum. Pathol.* **1992**, *23*, 1159−1166.

(17) Kawahara, E.; Ooi, A.; Nakanishi, I. Integrin distribution in gastric carcinoma: association of beta 3 and beta 5 integrins with tumor invasiveness. *Pathol. Int.* **1995**, *45*, 493−500.

(18) Albelda, S. M.; Mette, S. A.; Elder, D. E.; Stewart, R. M.; Damjanovich, L.; Herlyn, M.; Buck, C. A. Integrin Distribution in Malignant-Melanoma − Association of the Beta-3-Subunit with Tumor Progression. *Cancer Res.* **1990**, *50*, 6757−6764.

(19) Gingras, M. C.; Roussel, E.; Bruner, J. M.; Branch, C. D.; Moser, R. P. Comparison of Cell-Adhesion Molecule Expression between Glioblastoma-Multiforme and Autologous Normal Brain-Tissue. *J. Neuroimmunol.* **1995**, *57*, 143−153.

(20) Kumar, C. C.; Nie, H. M.; Rogers, C. P.; Malkowski, M.; Maxwell, E.; Catino, J. J.; Armstrong, L. Biochemical characterization of the binding of echistatin to integrin alpha(v)beta(3) receptor. *J. Pharmacol. Exp. Ther.* **1997**, *283*, 843−853.

(21) Achilefu, S.; Bloch, S.; Markiewicz, M. A.; Zhong, T. X.; Ye, Y. P.; Dorshow, R. B.; Chance, B.; Liang, K. X. Synergistic effects of light-emitting probes and peptides for targeting and monitoring integrin expression. *Proc. Natl. Acad. Sci. U.S.A.* **2005**, *102*, 7976−7981.

(22) Ye, Y.; Li, W. P.; Anderson, C. J.; Kao, J.; Nikiforovich, G. V.; Achilefu, S. Synthesis and characterization of a macrocyclic near-infrared optical scaffold. *J. Am. Chem. Soc.* **2003**, *125*, 7766−7767.

prepared in three steps consisting of solid-phase peptide synthesis, intramolecular lactamization in solution, and dye conjugation.[21] The following compounds were prepared:

Cypate−GRDSPK−OH (2): 8.1 mg; 6.40 μmol; 25.6% isolated yield; mass (calculated): 1265.3; observed (ES-MS): 1265.3 $[M]^+$.

Cypate−GRGDPK−OH (3): 6.4 mg; 4.84 μmol; 19.4% isolated yield; mass (calculated): 1322.37; observed (ES-MS): 1322.55 $[M]^+$.

Cyclo[RGDfVK(ϵ-cypate)] (4): f is D-phenylalanine: 3.7 mg; 12% isolated yield; ES-MS: 1309.47 $[MH]^+$; 655.29 $[M + 2H]^{2+}$.

Gly−Arg−Asp−Ser−Pro−Lys−OH (7): 19.92 mg; 19.9 μmol; 79.6% isolated yield; mass (calculated): 658.35; observed (ES-MS): 659.36 $[MH]^+$.

Cell Lines. The human nonsmall cell carcinoma cell line A549, the human glioblastoma cell line U87, the human embryonic kidney cell line HEK, and the human erythroblast cell line HEL were purchased from American Type Culture Collection (Manassas, VA). A549 cells were maintained in Ham's F12K medium supplemented with 2 mM L-glutamine, 1.5 g/L sodium bicarbonate, 10% fetal calf serum, 100 units/mL penicillin, and 100 units/mL streptomycin. U87 and HEK cells were maintained in minimum essential medium (MEM) with 2 mM L-glutamine and Earle's BSS adjusted to contain 1.5 g/L sodium bicarbonate, 0.1 mM nonessential amino acids, and 1.0 mM sodium pyruvate, with 10% fetal calf serum, 100 units/mL penicillin, and 100 units/mL streptomycin. HEL cells were maintained in RPMI 1640 with 2 mM L-glutamine adjusted to contain 1.5 g/L sodium bicarbonate, 4.5 g/L glucose, 10 mM HEPEs, and 1.0 mM sodium pyruvate. Vascular smooth muscle cells (VSMCs) from the aortas of $\beta3^{-/-}$apoE$^{-/-}$ and $\beta3^{+/+}$apoE$^{-/-}$ mice were provided by Dr. Clay F. Semenkovich (Washington University Medical School, St. Louis, MO). VSMCs were maintained in Dulbecco's modified Eagle's medium (DMEM) containing 10% fetal bovine serum, 4 mmol/L L-glutamine, 1 mM sodium pyruvate, 100 U/mL penicillin, 0.25 μg/mL amphotericin, and 100 μg/mL streptomycin. All of the cell lines were maintained in humidified atmosphere containing 5% CO$_2$ at 37 °C.

Receptor Binding Determination. A 96-well filtration plate was blocked with 0.1% polyethylenimine blocking solution by incubation overnight at 4 °C. ^{125}I-Echistatin (50 nmol/L) was added to the binding buffer (50 mM Tris-HCl, pH 7.4, 100 mM NaCl, 2 mM CaCl$_2$, 1 mM MgCl$_2$, 1 mM MnCl$_2$, 0.1% BSA) with integrin $\alpha_v\beta_3$ protein (50 ng/well in 96-well filtration plate) and ligands. The concentration range of ligand was between 0.01 and 100 μM. The mixture was incubated for 2 h by shaking at room temperature. Each well was washed three times with 0.25 mL of ice-cold binding buffer and dried. The filters were removed using a punch apparatus and counted in a gamma counter.[20]

Immunostaining. Cells grown on Lab-Tek slides were fixed in 3% paraformaldehyde in PBS for 30 min. After washing three times for 5 min each in PBS, the cells were blocked to mask nonspecific binding sites with PBS containing 1% normal goat serum (blocking solution) for 1 h. Primary antibodies of mouse anti-human α_V or β_3 integrin antibodies (Chemicon International, Temecula, CA.) or anti-human $\alpha_{IIb}\beta_3$ (GeneTex, Inc., South Bend, IN) diluted 1:500 (v/v) in blocking solution were added to each well and incubated overnight at 4 °C. After washing three times for 10 min each in PBS, cells were incubated for 1 h with diluted biotinylated-anti-mouse IgG antibody in blocking solution. After washing, antigens were detected with avidin-horseradish peroxidase conjugate and diamino benzidine (Vector Laboratories, Burlingame, CA). Slides were counterstained with Mayers Hematoxylin, and the cover slips were mounted for microscopic examination.

Western Blotting. A549 and HEL cells were harvested and lysed in CHAPS buffer (50 mM Pipes/HCl, pH 6.5, 5 mM dithiothreitol (DTT), 2 mM EDTA, 0.1% CHAPS, 20 μg mL^{-1} leupeptin, 10 μg mL^{-1} pepstatin, 10 μg mL^{-1} aprotinin, 1 mM phenyl methylsulfonyl fluoride). Cells were homogenized with an ultrasonic processor, and lysis was confirmed by microscopy. Total cell lysates were clarified by centrifugation. Protein concentration of the lysates was determined using the Bio-Rad protein assay reagent. SDS-PAGE was performed using the EC120 Mini vertical gel system (Thermo EC, Holbrook, NY). Electrophoresed samples were transferred onto PVDF membrane using an EC140 Mini Blot Module (Thermo EC, Holbrook, NY) apparatus. The membranes were blocked 1 h at room temperature in PBS containing 5% nonfat dry milk (w/v) and 0.1% (v/v) Tween-20 (PBS-T) after which they were incubated overnight in PBS-T containing 3% nonfat dry milk (w/v) and 1:1000 dilution of anti-β_3, anti-α_V, or anti-$\alpha_{IIb}\beta_3$ antibodies. After washing three times for 10 min each in PBS-T, membranes were incubated for 1 h with diluted polyclonal rabbit anti-goat IgG conjugated to horseradish peroxidase in PBS-T containing 3% nonfat dry milk (w/v). Membranes were again washed three times for 10 min each in PBS-T and developed using the chemiluminescence ECL kit (Pierce) according to the manufacturer's instruction.

Fluorescence and Confocal Microscopy. Cells were grown on Lab-Tek slides. The medium was replaced, and cells were incubated for various times up to 4 h at 37 °C in the presence of 1 μM dye conjugated peptides. For fluorescence microscopy, cells were visualized with an Olympus FV1000 microscope using 775/50 excitation, 845/55 emission filters. For antibody blocking studies, cells were pretreated for 30 min with 10 μg/mL functional blocking anti-α or

(23) Atherton, E.; Sheppard, R. C. *Solid-Phase Peptide Synthesis: A Practical Approach*; Oxford University Press: Oxford, England, 1989.

(24) Achilefu, S.; Dorshow, R. B.; Bugaj, J. E.; Rajagopalan, R. Novel receptor-targeted fluorescent contrast agents for in vivo tumor imaging. *Invest. Radiol.* **2000**, *35*, 479−485.

(25) Achilefu, S.; Jimenez, H. N.; Dorshow, R. B.; Bugaj, J. E.; Webb, E. G.; Wilhelm, R. R.; Rajagopalan, R.; Johler, J.; Erion, J. L. Synthesis, in vitro receptor binding, and in vivo evaluation of fluorescein and carbocyanine peptide-based optical contrast agents. *J. Med. Chem.* **2002**, *45*, 2003−2015.

anti-β antibodies from Molecular Probes (Eugene, OR). Relative fluorescence was determined for five different areas of each experimental condition using the Slidebook software, and the results were averaged. The average relative fluorescence for each condition was normalized to cells treated with **2**.

Molecular Modeling. Energy calculations for compounds Cyp−GRDSPK−OH (**2**), Cypate−GRGDPK−OH (**3**) and cyclo[RGDfVK(ϵ-cypate)] (**4**) were performed using the ECEPP/2 force field.[26,27] Dihedral angles were the only variables in the process of energy minimization because rigid valence geometry was assumed. Aliphatic and aromatic hydrogens were generally included in united atomic centers of CH_n type, and only H^α atoms were described explicitly. The dielectric constant value was 80.0 in order to dampen the strong electrostatic interaction between charged groups, thereby allowing exploration of a wider set of low-energy conformations. This precaution is essential, keeping in mind the considerable uncertainties involved in mimicking a heterogeneous protein environment (as in a complex with $\alpha_v\beta_3$ integrin). The valence geometry of the cypate group was determined employing the readily available SYBYL computational package, and the atomic charges on cypate were calculated in the Gasteiger−Huckel approximation.

Conformational sampling involved exploring all of the combinations of the local minima of the peptide backbone, including five combinations of (ϕ,ψ) dihedral angles for the non-Gly and non-Pro residues, namely, ($-140°$, $140°$), ($-75°$, $140°$), ($-75°$, $80°$), ($-60°$, $-60°$), and ($60°$, $60°$), which correspond to the local minima β, pII′, pII, γ′, α_R, and α_L in the Ramachandran plot. For the D-Phe residue, the same (ϕ,ψ) combinations with opposite signs of angles were used. For Pro residues, three (ϕ,ψ) combinations were used: ($-75°$, $140°$), ($-75°$, $80°$), and ($-75°$, $-60°$). For the Gly residue, the β, pII, γ′, α_R and α_L minima, and the minima symmetrical to β, pII, and γ′ were used, giving eight local minima. Also, the three possible rotations around all single bonds of **1** (i.e., of $60°$, $180°$, and $-60°$) were considered. Only trans amide bonds ($\omega = 180°$) were considered. For **4**, only the combinations of the ϕ, ψ, and ω angles resulting in a ring closure were selected as starting conformations for further energy minimization; that is, conformations with a distance $\leq$4 Å between the C^α atom of Arg[1] and the dummy atom corresponding to the Me atom in the Lys(ϵ-Cyp)[6]−NHMe construct. Totally, 97 601 conformations for compound **2**, 115 486 for **3**, and 62 492 for **4** were considered as starting points for energy minimization. Closing of the cycle was achieved using parabolic closing potentials with U_0 of 100 kcal/mol between the C^α and C' atoms of Arg[1] and the dummy atoms representing the Me

and C' atoms in the Lys(ϵ-Cyp)[6]−NHMe construct, respectively. The dihedral angle values of all side chain groups were optimized before energy minimization to achieve their most favorable spatial arrangements according to an algorithm described elsewhere.[28]

Low-energy conformations were selected according to criteria $\Delta E = E - E_{min} \leq 10$ kcal/mol. Redundant backbone conformations were subsequently removed. If one (or more) of the backbone torsional angles and rotations in **1** differed by more than $40°$ from the corresponding angle of a previous conformation, then the conformation was considered unique (nonredundant).

Animal Studies. All in vivo studies were performed in compliance with the Washington University Animal Study Committee's requirements for the care and use of laboratory animals in research. Nude mice were anesthetized with xylazine/ketamine cocktail via intraperitoneal injection and placed in a supine position. The nude mice ($18-22$ g) were injected subcutaneously with A549 cells (1×10^6) on the lower-left flank. Tumor masses were palpable at $5-7$ days post implant, which reached 5 mm in $10-15$ days. Prior to injection of the probe, the mice were anesthetized as described above. The molecular probes were dissolved in 20% aqueous DMSO and animals were injected retro-orbitally (29-gauge needle) with doses of 0.3 μmol/kg body weight. Injected volumes were 100 μL for each mouse. A time-domain diffuse optical imaging system and a planar fluorescence imager were used for noninvasive imaging of whole mice and ex vivo tissue parts, respectively, as described elsewhere.[21,29] At the completion of the study, the mice were euthanized and tissues were excised and rinsed with water. The tissues were placed under the CCD camera, and the fluorescence emission from each organ was measured after excitation with the 780 nm laser sources. Tissue parts, instead of whole organs, were used to minimize problems associated with depth-dependent nonlinear fluorescence emission. A statistical program in the WinView package was used to estimate the mean fluorescence intensity per tissue.

Results

Chemistry. Because the discovery that endogenous proteins such as fibronectin and vitronectin bind integrins through their RGD peptide sequence,[30,31] a variety of peptide and non-peptide analogues containing the RGD motif have

(26) Dunfield, L. G.; Burgess, A. W.; Scheraga, H. A. Energy Parameters in Polypeptides. 8. Empirical Potential Energy Algorithm for the Conformational Analysis of Large Molecules. *J. Phys. Chem.* **1978**, *82*, 2609−2616.

(27) Nemethy, G.; Pottle, M. S.; Scheraga, H. A. Energy Parameters in Polypeptides. 9. Updating of Geometrical Parameters, Nonbonded Interactions, and Hydrogen Bond Interactions for the Naturally Occurring Amino Acids. *J. Phys. Chem.* **1983**, *87*, 1883−1887.

(28) Nikiforovich, G. V.; Hruby, V. J.; Prakash, O.; Gehrig, C. A. Topographical Requirements for Delta-Selective Opioid Peptides. *Biopolymers* **1991**, *31*, 941−955.

(29) Bloch, S.; Lesage, F.; McIntosh, L.; Gandjbakhche, A.; Liang, K.; Achilefu, S. Whole-body fluorescence lifetime imaging of a tumor-targeted near-infrared molecular probe in mice. *J. Biomed. Opt.* **2005**, *10*, 54003.

(30) Pierschbacher, M. D.; Ruoslahti, E. Cell attachment activity of fibronectin can be duplicated by small synthetic fragments of the molecule. *Nature* **1984**, *309*, 30−33.

(31) Charo, I. F.; Nannizzi, L.; Smith, J. W.; Cheresh, D. A. The Vitronectin Receptor Alpha-V-Beta-3 Binds Fibronectin and Acts in Concert with Alpha-5-Beta-1 in Promoting Cellular Attachment and Spreading on Fibronectin. *J. Cell Biol.* **1990**, *111*, 2795−2800.

Table 1

compd	structure	IC$_{50}$ ± SD (μM)
1	cypate[a]	not applicable[b]
2	cypate-GRDSPK−OH	not applicable[b]
3	cypate-GRGDSPK−OH	10.66 ± 1.87
4	cyclo[RGDf VK(ϵ-cypate)]	79.09 ± 3.03
5	cyclo[RGDfV]	0.113 ± 0.008
6	cyclo[RGDfVK]	1.926 ± 0.347

[a] Structure of cypate moiety:
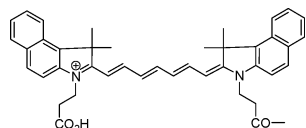
[b] Values of IC50 >100 μM were not determined because of the limitation of the assay protocol.

been developed.[32,33] In this study, we evaluated the effect of rearranging the tripeptide sequence by investigating compounds listed in Table 1. The compounds included a cypate-labeled linear GRD peptide (**2**) as well as the analogous linear (Cypate-GRGDSPK−OH, **3**) and cyclic (cyclo[RGDfVK-(ϵ-cypate)], **4**; cyclo[RGDfV], **5**; and cyclo[RGDfVK], **6**) RGD compounds for comparative study. All peptides were prepared on solid supports by standard Fmoc chemistry.[23] These peptides were labeled with **1**, which fluoresces in the NIR wavelengths. The absorption of photons by tissues is low in the NIR region, allowing deeper penetration of light in tissue.[34] Therefore, labeling molecules with **1** facilitates the use of the same compound for microscopy and in vivo optical imaging studies. Tests of homogeneity, identity, and purity were conducted by spectral analysis, LC-MS, and different HPLC conditions. Typically, all compounds used for biological assays were >95% pure by HPLC analysis. Expectedly, the isolated yields of the linear compounds were more than 3 times higher than their cyclic analogues.

Western Blotting. The presence of $\alpha_{\text{IIb}}\beta_3$ and $\alpha_{\text{v}}\beta_3$ in the A549 cells was verified by Western blot. Both α_{v} and β_3 are expressed in the cell line (Figure 1), consistent with previous reports.[35,36] Previous studies have shown that β_3 protein dimerizes only with either α_{v} or α_{IIb} integrins.[4] Therefore, we also tested A549 for the expression of $\alpha_{\text{IIb}}\beta_3$, using HEL cells as positive control.[37,38] As shown in Figure 1c, the dimeric $\alpha_{\text{IIb}}\beta_3$ is present in this cell line.

Receptor-Binding Studies. The receptor binding affinities of compounds **2**−**6** (Table 1) were evaluated by using purified ABIR proteins, ^{125}I-echistatin, and compound **5** as
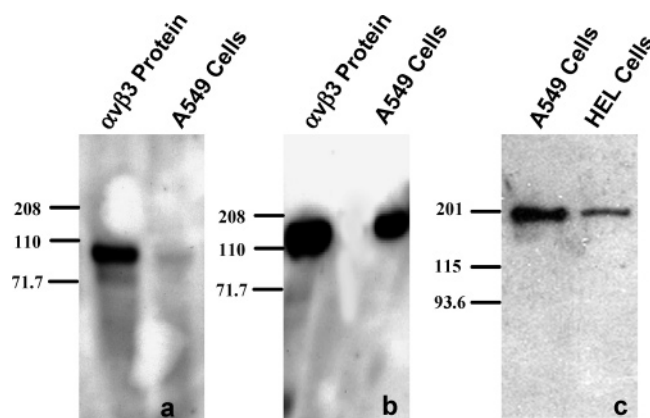

Figure 1. Identification of integrins in A549 and HEL cells by Western blot. Proteins and membranes were probed with (a) anti-α_{v}, (b) anti-β_3, and (c) anti-$\alpha_{\text{IIb}}\beta_3$ antibodies. Integrin $\alpha_{\text{V}}\beta_3$ protein (1.8 μg) and A549 cell membrane proteins (38 μg) were loaded in each lane in a and b. In c, A549 (50 μg) and HEL (50 μg) cell membrane proteins were loaded in each lane. HEL cells served as positive control for $\alpha_{\text{IIb}}\beta_3$ integrin proteins.

the target receptor, tracer, and reference standard, respectively. Echistatin is a polypeptide that binds purified ABIR specifically and irreversibly and the radiolabeled analogue is used widely in ABIR binding assays.[20,39] All of the RGD compounds were recognized by ABIR, with the exception of **2**, which had IC$_{50}$ of >100 μM (Table 1). The highest binding affinity (IC$_{50}$ ca. 0.11 μM) was found for the RGD peptide cyclo[RGDfV] (**5**), which is in agreement with the literature data (IC$_{50}$ ca. 0.05 μM).[40] Because of the rearrangement of the RGD peptide sequence, the low binding of Cyp-GRD peptide to ABIR was expected. Considering that in vivo studies showed enhanced retention of **2** in A549 tumor tissue despite its low affinity for the heterodimeric ABIR proteins, we further performed the binding assay using A549 cell membranes. We did not observe any improvement in the ABIR binding affinity by this method.

(32) Aumailley, M.; Gurrath, M.; Muller, G.; Calvete, J.; Timpl, R.; Kessler, H. Arg-Gly-Asp constrained within cyclic pentapeptides. Strong and selective inhibitors of cell adhesion to vitronectin and laminin fragment P1. *FEBS Lett.* **1991**, *291*, 50−54.

(33) Gurrath, M.; Muller, G.; Kessler, H.; Aumailley, M.; Timpl, R. Conformation/activity studies of rationally designed potent anti-adhesive RGD peptides. *Eur. J. Biochem.* **1992**, *210*, 911−921.

(34) Hawrysz, D. J.; Sevick-Muraca, E. M. Developments toward diagnostic breast cancer imaging using near-infrared optical measurements and fluorescent contrast agents. *Neoplasia* **2000**, *2*, 388−417.

(35) Triantafilou, M.; Triantafilou, K.; Wilson, K. M.; Takada, Y.; Fernandez, N. High affinity interactions of coxsackievirus A9 with integrin alpha v beta 3 (CD51/61) require the CYDMKTTC sequence of beta 3, but do not require the RGD sequence of the CAV-9 VP1 protein. *Hum. Immunol.* **2000**, *61*, 453−459.

(36) Odrljin, T. M.; Haidaris, C. G.; Lerner, N. B.; Simpson-Haidaris, P. J. Integrin alpha v beta 3-mediated endocytosis of immobilized fibrinogen by A549 lung alveolar epithelial cells. *Am. J. Respir. Cell Mol. Biol.* **2001**, *24*, 12−21.

(37) Tabilio, A.; Rosa, J. P.; Testa, U.; Kieffer, N.; Nurden, A. T.; Del Canizo, M. C.; Breton-Gorius, J.; Vainchenker, W. Expression of platelet membrane glycoproteins and alpha-granule proteins by a human erythroleukemia cell line (HEL). *EMBO J.* **1984**, *3*, 453−459.

(38) Jin, Y.; Wilhide, C. C.; Dang, C.; Li, L.; Li, S. X.; Villa-Garcia, M.; Bray, P. F. Human integrin beta3 gene expression: evidence for a megakaryocytic cell-specific cis-acting element. *Blood* **1998**, *92*, 2777−2790.

(39) Wong, A.; Hwang, S. M.; McDevitt, P.; McNulty, D.; Stadel, J. M.; Johanson, K. Studies on alpha(v)beta(3)/ligand interactions using a [H-3]SK&F-107260 binding assay. *Mol. Pharmacol.* **1996**, *50*, 529−537.
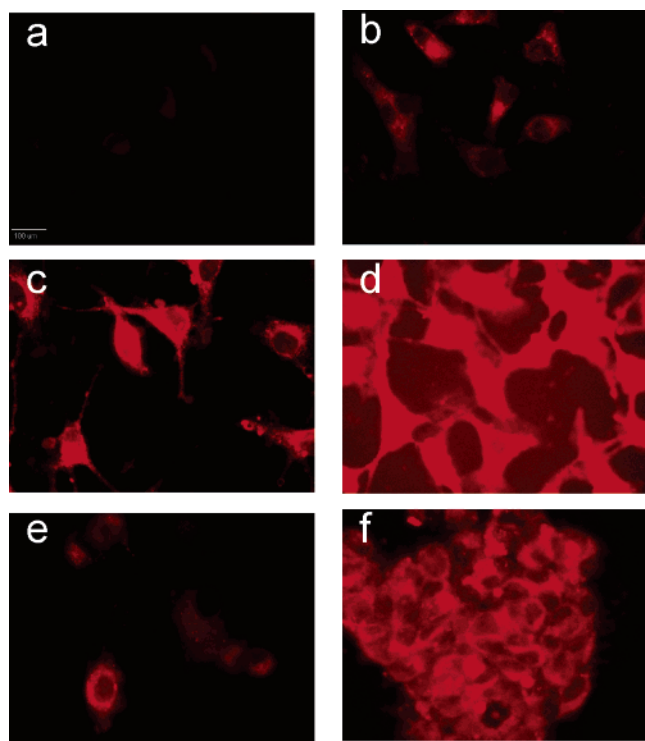
Figure 2. Internalization of various compounds in ABIR-positive A549, U87, and HEK cells at 37 °C. A549 cells were treated with 1 μM of (a) **1**, (b) **2**, (c) **3**, and (d) **4** for 4 h or with **2** for 1 h using (e) U87 and (f) HEK cells.

Cell Uptake and Internalization of Dye−Peptide Conjugates. The ABIR-positive cells were incubated with **1** and its peptide conjugates at 37 °C for different time points. High accumulation was observed for the compounds at 4 h postincubation relative to earlier time points. All fluorescence intensities were normalized to that of **1** as background (Figure 2a). As was expected, all of the bioconjugates internalized in the cells. However, no clear correlation between the binding affinities of the compounds to ABIR and their fluorescence intensities in cells was observed. On one hand, linear RGD compound **3** with higher affinity showed higher intensity than linear GRD compound **2** with low affinity (compare Figure 2b and c). On the other hand, the cyclic RGD compound **4** (Figure 2d) showed much higher fluorescence intensity than linear RGD compound **3** (Figure 2c), although the ABIR binding affinities of both compounds to ABIR were comparable (Table 1). Additional testing of **2** in other ABIR-positive cells (U87, HEK)[41,42] also showed internalization of the compound within an hour of incubation (Figure 2e and f). The uptake of **2** in these cells was not anticipated based on its low ABIR binding affinity. Most importantly, co-incubation of **2** with the ABIR-avid peptide **5** (compound with the highest affinity to ABIR in Table 1)
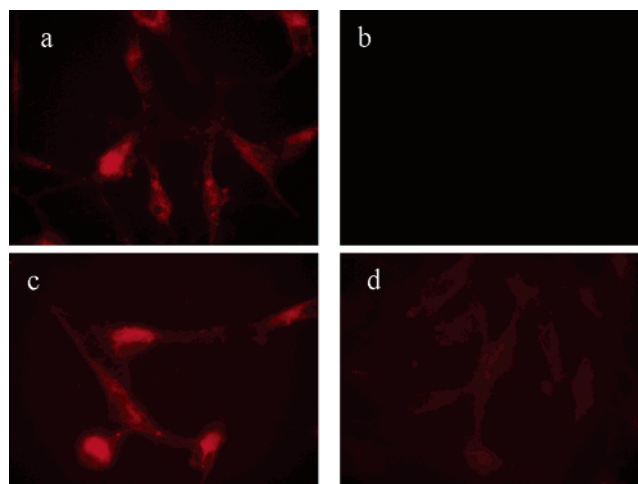
Figure 3. A549 cells preincubated for 15 min with peptide or 30 min with antibodies or with **2** alone. Cells were incubated with (a) **2** alone, (b) **2** with **5**, (c) **2** with anti-α_v, and (d) **2** with anti-β_3.

blocked the uptake of all of the compounds (data for **2** is shown in Figure 3b), suggesting the recognition of the bioconjugates by the same receptor.

To assess the roles of different integrins in the cellular internalization of **2** in ABIR-positive cells, we incubated A549 cells with functional blocking antibodies to different α and β integrins prior to adding **2**. As shown in Figure 3c, blocking of α_v integrin by the specific antibody did not inhibit the internalization of **2**. We found also that, with the exception of anti-β_3 integrin antibody (Figure 3d), all of the other anti-β integrin antibodies tested were not effective in inhibiting the uptake of **2** by A549 cells. The successful blocking of cellular internalization of **2** by the anti-β_3 integrin antibody (Figure 3) suggests that **2** binds to β_3 integrin and that this interaction may mediate the observed internalization.

Immunostaining for α_v, α_{IIb}, β_3, and the Heterodimers in Cells Treated with Compound 2. To confirm the receptors that mediate internalization of **2** in A549 cells, we assessed the levels of α_v, β_3, $\alpha_v\beta_3$, and $\alpha_{IIb}\beta_3$ protein in treated and untreated cells by immunostaining. The results show that all of the antibodies stained untreated A549 cells (Figure 4). Relative to the PBS treated cells, preincubation in buffer containing **2** resulted in reduced staining of A549 cells with the anti-α_v, anti-β_3, $\alpha_v\beta_3$, and the $\alpha_{IIb}\beta_3$ antibodies.

Assessment of the Internalization of Compounds 2 and 4 in Integrin β_3 Knockout Cells. Having shown that **2** preferentially binds to β_3 integrin in ABIR-positive cells, we

(40) Pfaff, M.; Tangemann, K.; Muller, B.; Gurrath, M.; Muller, G.; Kessler, H.; Timpl, R.; Engel, J. Selective recognition of cyclic RGD peptides of NMR defined conformation by alpha IIb beta 3, alpha V beta 3, and alpha 5 beta 1 integrins. *J. Biol. Chem.* **1994**, *269*, 20233−20238.

(41) Ling, W. L. W.; Longley, R. L.; Brassard, D. L.; Armstrong, L.; Schaefer, E. J. Role of integrin alpha(v)beta(3) in the production of recombinant adenoviruses in HEK-293 cells. *Gene Ther.* **2002**, *9*, 907−914.

(42) Bello, L.; Lucini, V.; Giussani, C.; Carrabba, G.; Pluderi, M.; Scaglione, F.; Tornei, G.; Villani, R.; Black, P. M.; Bikfalvi, A.; Carroll, R. S. IS201, a specific alpha v beta 3 integrin inhibitor, reduces glioma growth in vivo. *Neurosurgery* **2003**, *52*, 177−185.
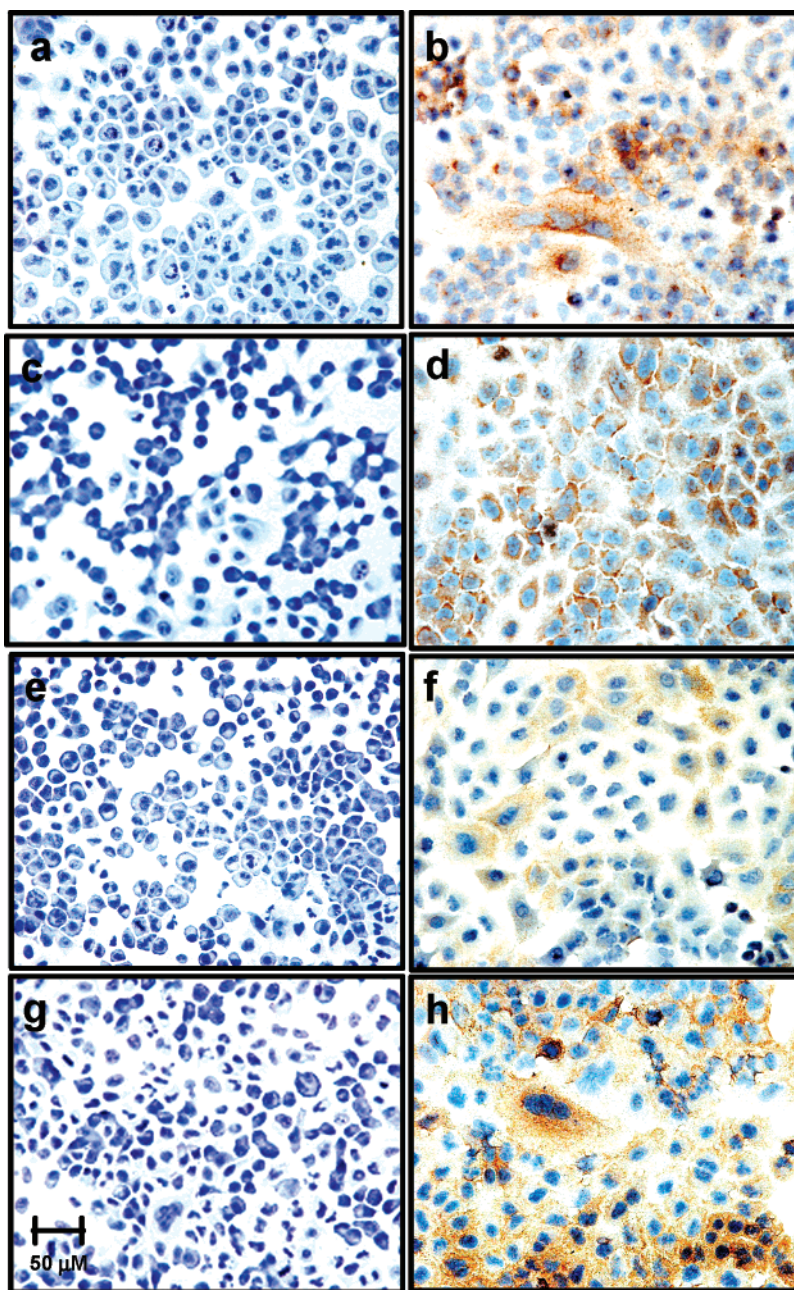
Figure 4. Immune staining of α_v (a and b), β_3 (c and d), $\alpha_{IIb}\beta_3$ (e and f), and $\alpha_v\beta_3$ (g and h) protein expression in A549 cells. Cells were treated with 100 μM of **2** (a, c, e, and g) or PBS (b, d, f, and h) for 1 h at 37 °C. Anti-α_v, anti-β_3, anti-$\alpha_{IIb}\beta_3$, and anti-$\alpha_v\beta_3$ integrin antibodies were used to identify the respective proteins.

hypothesized that it would not internalize in β_3 knockout cells. Accordingly, we compared the internalization of compounds **2** and **4** in vascular smooth muscle cells (VSMC) of the integrin β_3 knockout cells and the wild-type. Expectedly, both compounds internalized in VSMC wild-type cells (Figure 5b and d), but the internalization of **2** was not observed in the β_3 knockout cells (Figure 5c). The fluorescence observed in Figure 5a is attributed to the binding of **4** with the α_v subunit. These findings further confirm that β_3 integrin actively mediated the cellular internalization of **2**.

Molecular Modeling. Energy calculations revealed 3155, 2434, and 133 nonredundant low-energy conformations for

2, **3**, and **4**, respectively. To evaluate the possibility of forming complexes with ABIR in the same binding mode as a known ABIR-avid RGD peptide, these compounds were compared to the "template" conformation of cyclo(RGDf-NMeV), whose complex with ABIR has been resolved in high resolution by X-ray crystallography.[43]

Geometrical comparison showed that some of the low-energy conformations of **2** (15 out of 3155) are similar to

(43) Xiong, J. P.; Stehle, T.; Zhang, R.; Joachimiak, A.; Frech, M.; Goodman, S. L.; Arnaout, M. A. Crystal structure of the extracellular segment of integrin alpha Vbeta3 in complex with an Arg-Gly-Asp ligand. *Science* **2002,** *296,* 151–155.
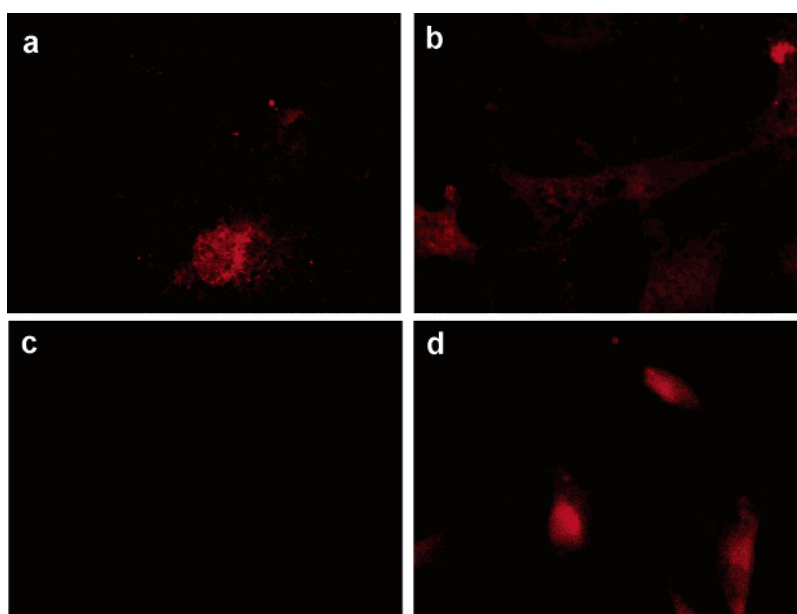
Figure 5. Vascular smooth muscle cells (VSMC) of integrin $\beta3$ knockout (a and c) and wild-type (b and d) mice were treated with 1 μM of **4** (a and b) and **2** (c and d) for 1 h at 37 °C.
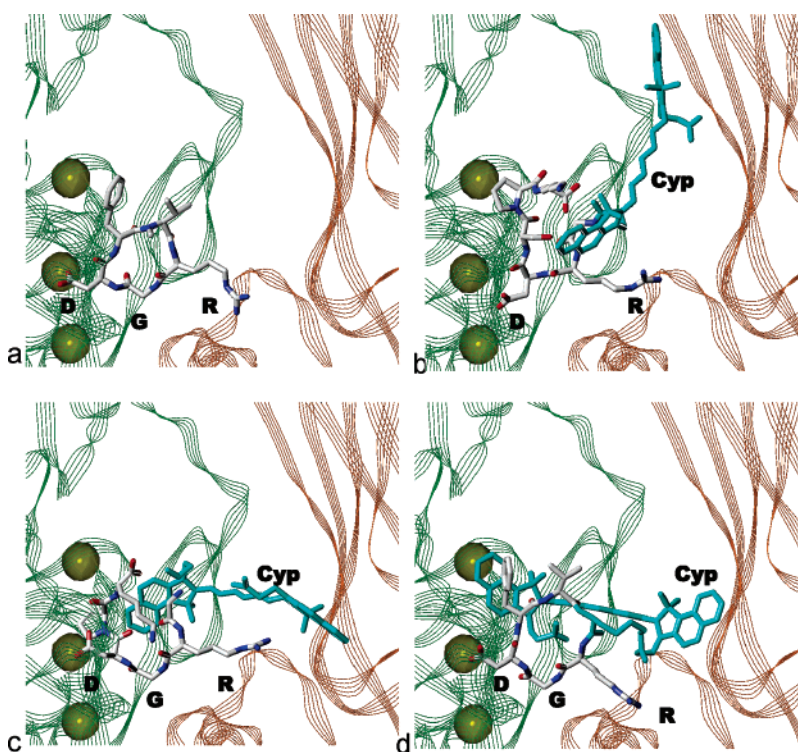

Figure 6. Representative conformations of RGD related compounds in complexes with $\alpha_V\beta_3$ integrin: (a) cyclo(RGDf-NMeV), (b) **2**, (c) **3**, and (d) **4**. All hydrogens are omitted. The cypate moiety **1** and residues it is attached to are shown in cyan. Residues involved in the RGD motifs and moieties **1** are labeled. α_V subunit of $\alpha_V\beta_3$ integrin is shown as line ribbon in orange, and the β_3 subunit is shown as line ribbon in green. Three Mn^{2+} ions in the β_3 subunit are shown as semi-transparent spheres in yellow.

the template conformation of cyclo(RGDf-NMeV) in complex with ABIR by overlapping Cα atoms of the GRDS fragment in **2** to the same atoms for residues NMeV, R, D, and f in cyclo(RGDf-NMeV); the corresponding root-mean-square (rms) values were less than 1.1 Å. In addition, some of the conformations (5 out of 15) that overlapped with the

template compound provided spatial arrangements of the cypate moiety without sterical clashes with ABIR molecule (i.e., all distances between the cypate moiety and ABIR atoms were less than 2 Å). Figure 6b displays a representative conformation of **2** in the complex with ABIR. General spatial orientation of compound **2** in Figure 6b is somewhat different
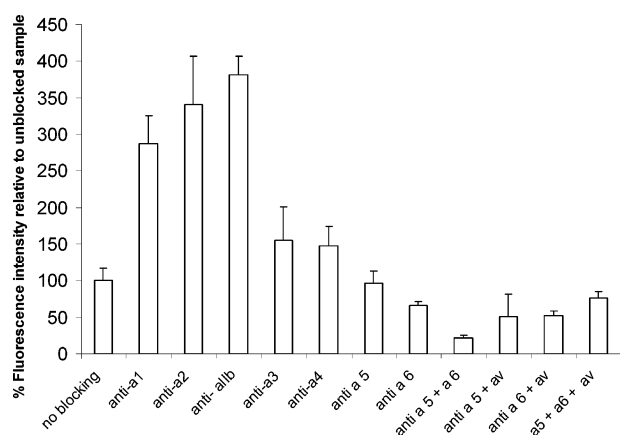
Figure 7. Relative fluorescence of A549 cells incubated with **2** with or without pretreatment with function blocking antibodies.

from that of cyclo(RGDf-NMeV) in Figure 6a, which is consistent with the much lower affinity of **2** binding to ABIR.

The ratio of the low-energy conformations of the linear RGD compound **3** compatible with the template conformation is significantly higher (631 out of 2434 conformations within the rms value cutoff less than 1.0 Å by overlapping Cα atoms of the fragments GRGD and NMeV-RGD) than **2**. Similarly, there are also more conformations (34 out of 631) without steric clashes of the cypate moiety with the ABIR for **3**. These findings agree with higher affinity of **3** to ABIR compared to that of **2**. The representative structure of **3** in complex with ABIR is shown in Figure 6c.

An even larger percentage of low-energy conformations of the cyclic RGD **4** (37 out of 133) is compatible with the template conformation within the rms cutoff less than 1.0 Å (comparison of the Cα atoms of the fragments RGDf in both compounds, **4** and cyclo(RGDf-NMeV)). However, only few of these conformations (3 out of 133) provide spatial arrangements for the cypate moiety without steric clashes with the ABIR molecule at the level of all cypate−ABIR atom−atom distances less than 1.5 Å. At the level of 2 Å accepted in the previous cases (see above), none of the confor-

mations are devoid of potential clashes with $\alpha_V\beta_3$ integrin. This observation may explain the decreasing affinity to ABIR from 1.9 μM for **6** to 79 μM for **4**, which differ from **6** only by addition of the cypate moiety to the side chain of the lysine residue (Table 1). The representative conformation of **4** is shown in Figure 6d. Generally, the results of molecular modeling agree with the experimental data on receptor binding affinity and support the assumption that compounds **2**, **3**, and **4**, which are the relatively weak binders, may bind to ABIR at the same site as the high-affinity ABIR binders such as cyclic RGD peptides **5** and cyclo(RGDf-NMeV).

Optical Imaging. The transparency of nude mice under near-infrared light enabled us to use the same molecular probes for both in vitro and in vivo studies. A time-domain diffuse optical tomography system[29] was used for the noninvasive optical imaging. Tissues were analyzed ex vivo by a planar fluorescence imaging system.[21] Laser sources operating at 780 nm excitation wavelength were used, and the fluorescence emission was detected at 830 nm. At 24 h postinjection, compounds **2**, **3**, and **4** preferentially localized in the ABIR-positive A549 tumors grown in nude mice (Figure 8). Unlike RGD compounds **3** and **4**, GRD-containing dye conjugate **2** had higher uptake in the tumor tissue. Interestingly, the retention of **2** in nontarget tissues, including the major excretion organs (liver and kidneys), were much lower than **3** and **4**. The superior clearance profile of **2** provides a strategy to image the expression of β_3 integrins in vivo.

As in the in vitro studies, the tumor uptake of **2** can be inhibited by ABIR-avid peptides such as **5**. For example, an equimolar amount of **5** blocked the uptake of **2** in A549 tumor-bearing mice (data not shown). Typically, higher concentrations ($>100\times$) of the blocking peptides were needed to inhibit the retention of compounds by a common receptor.[44] Therefore, the small dose of **5** needed to block the uptake of **2** confirmed the low binding affinity of **2** to ABIR. However, the weak ligand−receptor interaction does not appear to decrease the uptake of **2** in tumors. This surprising observation could be explained by the preponder-
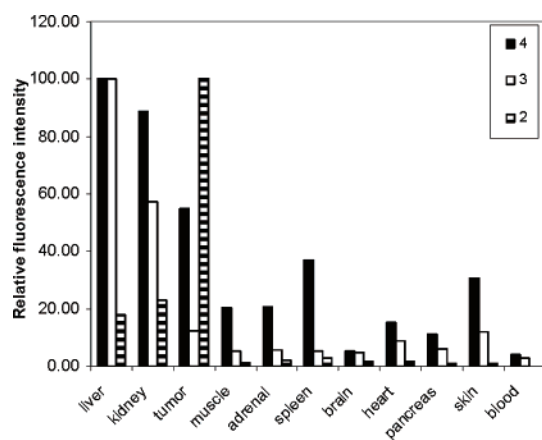
(a)
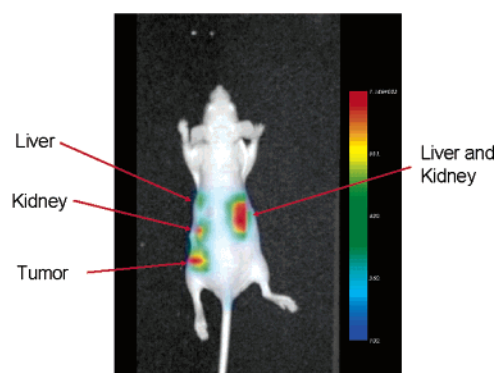
(b)

Figure 8. Biodistribution of compounds in A549 tumor-bearing nude mice at 24 h postinjection. (a) Distribution of **2**, **3**, and **4** in different tissues. (b) Whole-body noninvasive optical imaging of the distribution of **2** in nude mice.

ance of the activated form of β_3 in the in vivo tumor model or the activation of β_3 subunit by **2**. Subsequent studies showed that **5** was unable to displace **2** in A549 tumor in mice 24 h postinjection of **2**. This suggests that **2** was not retained on the tumor cell membranes but probably internalized in the tumor cells by β_3 integrin receptor. Thus, the superior biodistribution profile of **2** in vivo provides a strategy to image and monitor the functional status of β_3 integrin in cells and live animals. The use of NIR fluorescent probes allows the assessment of molecular processes in cells and intact animals without changing the fluorescent labels.

Discussion

The roles of heterodimeric integrins and their subunits have been well documented, and new insight into the mechanisms of their biological activities continues to be unraveled.[45,46] Although the individual integrins are known to exert specific biological effects, little effort has been made to design synthetic ligands that target integrin receptor subunits. NIR dye-labeled linear hexapeptide **2**, whose RGD sequence was rearranged to GRD, showed unexpectedly high uptake in ABIR-positive tumor tissue in vivo.[21] It was shown that at 24 h postinjection, compounds **2**, **3**, and **4** preferentially localized in the ABIR-positive A549 tumors grown in nude mice. Unlike RGD compounds **3** and **4**, GRD compound **2** had higher uptake in the tumor tissue.[21] Interestingly, the retention of **2** in nontarget tissues was much lower than **3** and **4**. As in the present in vitro studies, the tumor uptake of **2** was inhibited by the ABIR-avid peptides such as **5**. Further studies showed that **5** was unable to displace **2** in A549 tumor in mice when administered 24 h postinjection of **2**. This suggests that **2** was not available for displacement by **5** because it was probably internalized by the tumor cells at 24 h postinjection.

On the basis of the high tumor retention of **2** in ABIR-positive tumors[21] and successful inhibition of its uptake by **5** (Figure 3), the binding affinity of the molecular probe to ABIR was expected to be high. However, the affinity was low in the receptor-binding assay and did not correlate with the observed uptake in vivo. A closer analysis of the in vivo blocking studies revealed that only an equimolar amount of **5** was needed to inhibit the uptake of **2**,[21] in contrast to the severalfold excess typically used in similar receptor blocking studies.[44] The ease of displacing **2** by **5** suggested that **2** may be interacting weakly with ABIR. However, this weak affinity of **2** for the heterodimeric ABIR proteins does not

appear to decrease the cellular internalization and uptake of **2** in ABIR-positive tumors. These observations point to a mechanism of molecular recognition that may not involve simultaneous interaction of **2** with both α_v and β_3 integrin subunits. For this reason, additional studies were performed to clarify the mechanism of **2** retention in ABIR-positive cells and tumors.

If **2** indeed has the propensity to bind an active site in the β_3 subunit, then it is interesting to evaluate which types of the heterodimeric integrin proteins are involved in binding. The tumor cell line used may express either one or both of the heterodimeric forms of β_3, $\alpha_v\beta_3$, and $\alpha_{IIb}\beta_3$. Western blot analysis indicated that the $\alpha_{IIb}\beta_3$ dimer and the α_v and β_3 subunits are expressed in the A549 tumor cells used in this study (Figure 1). The observed expression of α_{IIb} in A549 cells contradicts a recent report that alludes to the exclusive expression of this protein in megakaryocytes and platelets.[47] Our finding is further supported by Chen et al.[48] who found α_{IIb} protein in a number of tumor cell lines. Subsequent testing in other ABIR-positive cell lines (Figure 2) confirmed the uptake of **2**, albeit to different extents that may reflect the functional status of the integrins.

Further studies with functional anti-integrin antibodies supported the hypothesis that the β_3 subunit possibly mediated the cell internalization of **2**. Comparative analysis of the internalization of **2** and **4** in the β_3-knockout and wild-type mouse cell line (VSMC) demonstrated that the deletion of β_3 decreased, if not eradicated, internalization of **2** in the β_3-knockout cells relative to the wide type (Figure 5). These results imply that the presence of the β_3 integrin is critical for the molecular recognition of **2**. Additional support for this pathway could be gleaned from the inhibition of anti-β_3 antibody staining by **2** in the immunocytochemical staining, which suggests that both **2** and the antibody may interact with the same binding site of β_3. Because this integrin dimerizes with α_v or α_{IIb}, internalization of the β_3-compound **2** complex will also result in a reduction in the staining of α_v, α_{IIb}, and the β_3 heterodimers, as shown in Figure 4. The result suggests that **2** binds to the β_3 integrin subunit, independent of the dimeric α subunit. Although β_3 expression is typically associated with the α subunits, numerous studies have shown that β_3 integrin alone can be up-regulated by a variety of biological or chemical factors such as sex hormones, vitamin D, and retinoic acid.[38] Furthermore, the unexpected enhanced uptake of **2** relative to **3** and **4** in A549 tumor-bearing mice[21] indicates that the β_3 integrin in this tumor model may recognize **2** more effectively than the related RGD compounds tested, which preferably interacts with the active sites of both α_v and β_3 protein receptors.

(44) Wu, Y.; Zhang, X.; Xiong, Z.; Cheng, Z.; Fisher, D. R.; Liu, S.; Gambhir, S. S.; Chen, X. microPET imaging of glioma integrin {alpha}v{beta}3 expression using (64)Cu-labeled tetrameric RGD peptide. *J. Nucl. Med.* **2005,** *46,* 1707−1718.

(45) Slack-Davis, J. K.; Parsons, J. T. Emerging views of integrin signaling: implications for prostate cancer. *J. Cell Biochem.* **2004,** *91,* 41−46.

(46) Paulhe, F.; Manenti, S.; Ysebaert, L.; Betous, R.; Sultan, P.; Racaud-Sultan, C. Integrin function and signaling as pharmacological targets in cardiovascular diseases and in cancer. *Curr. Pharm. Des.* **2005,** *11,* 2119−2134.

(47) Fang, B. J.; Zheng, C. M.; Liao, L. M.; Han, Q.; Sun, Z.; Jiang, X. Y.; Zhao, R. C. H. Identification of human chronic myelogenous leukemia progenitor cells with hemangioblastic characteristics. *Blood* **2005,** *105,* 2733−2740.

(48) Chen, Y. Q.; Trikha, M.; Gao, X. A.; Bazaz, R.; Porter, A. T.; Timar, J.; Honn, K. V. Ectopic expression of platelet integrin alpha IIb beta 3 in tumor cells from various species and histological origin. *Int. J. Cancer* **1997,** *72,* 642−648.

Compound **2** possesses a linear peptide whose structural flexibility may allow it to associate with different kinds of integrin subunits through conformational changes. Therefore, we employed extensive energy calculations to evaluate the recognition of **2** by ABIR. Molecular modeling confirmed the assumption that compounds **2**, **3**, and **4** may bind to ABIR in the mode displayed in Figure 6, which allowed us to calculate the distribution of residue−residue contacts between the ligands and two subunits of molecule. While the template ligand cyclo(RGDf-NMe-V) features 4 contacts with α_v subunit and 17 contacts with β_3 subunit (the residue−residue contact is defined as Cα−Cα distance less than 8 Å [49]), the numbers of corresponding contacts were 1 and 16, respectively for **2**, and 4 and 23 for **3**. The ratios of these numbers clearly favor interaction of **2** with the β_3 integrin, rather than with the α_v integrin, being in close agreement with the obtained experimental data.

The bulk of our experimental and modeling data emphasizes interaction with the β_3 integrin as the primary mechanism of the uptake of **2** by tumors. However, our additional data suggest that some aspects of this mechanism deserved additional investigation. The β_3 integrin is known to dimerize only with either α_v or α_{IIb} integrin subunits in physiological environment.[50] We have shown that anti-α_v antibody did not inhibit the internalization of **2** (Figure 3c). A similar test performed with anti-α_{IIb} antibody enhanced the uptake of **2** (Figure 7). This observation is not entirely surprising because molecular interaction of the antibody with α_{IIb} can activate β_3 if the binding favors the separation of the cytoplasmic α and β domains.[51] A caveat in this analysis is that the anti-α_{IIb} antibody used has not been tested for functional blocking at the time of this study. To further evaluate this observation, we tested the effects of some commercially available functional blocking antibodies specific for various α integrins on the internalization of **2** (Figure 7). Although anti-α_v and anti-α_5 antibodies had no significant effect on the cellular uptake of **2** by A549 cells, pretreatment with the antibodies to the α_1, α_2, and α_{IIb} proteins resulted in a substantial increase in the internalization of **2**, whereas the anti-α_3 and anti-α_4 antibodies induced a slight increase. Interestingly, pretreatment with anti-α_6 antibody partially inhibited the internalization of **2**. This decrease was not expected for α_6 because it is not known to dimerize with β_3. Therefore, the partial inhibition of the internalization of **2** by anti-α_6 antibody suggests that other integrins may regulate the activity of the β_3 subunit.[50] To test this hypothesis, A549 cells were pretreated with a combination of anti-α integrin antibodies.

When anti-α_5 and anti-α_6 were used together, inhibition of internalization was greater than when each antibody was used alone. When the anti-α_5 and anti-α_6 antibodies were used in combination with antibody to α_v, a reversal of the blocking effects of the pretreatment with combined anti-α_5 and anti-α_6 antibodies was observed. This demonstrates that the α_v integrin reduces the inhibitory effect of the other integrins on the cellular internalization of **2**, although a combination of α_5 with either α_v or α_6 appears to enhance blocking of the internalization. The complex effects of the antibodies on the internalization of **2** could be useful in formulating GRD compounds for in vivo applications. For example, if the addition of anti-α_1, α_2, or α_{IIb} antibody results in the activation of β_3 integrin in cancer cells, pre-administration of the antibody before injection of **2** or its derivatives may enhance tumor localization and treatment.

Although not the central focus of this study, we observed that the internalization by A549 cells (Figure 2) and uptake by tumor tissue (Figure 8) were higher for **4** than **3**, despite the higher receptor binding affinity of **3** compared with **4** (Table 1). It is likely that the structurally constrained cyclic peptides retained their optimal receptor binding conformation, whereas the flexible linear peptide had many nonbinding conformations under the incubation or in vivo conditions. This could be explained further by the molecular modeling results that showed a larger percentage of low-energy conformations of the cyclic RGD **4** than linear compound **3**, which could translate to higher retention in ABIR-positive cells and tissues. In contrast, the in vitro low receptor-binding affinity of **4** relative to **3** by using purified proteins reflects the sterical clashes caused by cypate upon conjugation with **4**. Therefore, the steric effect of cypate is likely negated by the large percentage of low-energy conformations of **4** that can bind ABIR-positive cells and tissues.

In summary, our findings strongly suggest that we have discovered a new molecular construct based on the linear peptide containing GRD sequence that preferentially targets the β_3 integrin. The superior biodistribution profile of this compound in vivo provides a strategy to image and monitor the functional status of the β_3 integrin in cells and live animals. The use of NIR fluorescent probes allows the assessment of molecular processes in cells and living animals without changing the fluorescent labels. Because of the upregulation of β_3 expression in cervical cancer and the accessibility of this organ to optical imaging, the use of **2** and its analogues provides a reliable method for detecting or imaging the early manifestation of cervical cancer. Additionally, the involvement of the β_3 integrin in a large number of pathologies suggests that the GRD template could be useful for evaluating the efficacy of anti-β_3 drugs in drug development.

(49) Galaktionov, S.; Nikiforovich, G. V.; Marshall, G. R. Ab initio modeling of small, medium, and large loops in proteins. *Biopolymers* **2001**, *60*, 153−168.

(50) Springer, T. A.; Wang, J. H. The three-dimensional structure of integrins and their ligands, and conformational regulation of cell adhesion. *Adv. Protein Chem.* **2004**, *68*, 29−63.

(51) Li, W.; Metcalf, D. G.; Gorelik, R.; Li, R.; Mitra, N.; Nanda, V.; Law, P. B.; Lear, J. D.; Degrado, W. F.; Bennett, J. S. A push−pull mechanism for regulating integrin function. *Proc. Natl. Acad. Sci. U.S.A.* **2005**, *102*, 1424−1429.